DOI: 10.1002/smll.200600112

# Parallel Manipulation of Bifunctional DNA Molecules on Structured Surfaces Using Kinesin-Driven Microtubules

*Cerasela Zoica Dinu, Jörg Opitz, Wolfgang Pompe, Jonathon Howard, Michael Mertig,* and Stefan Diez**

*We have developed a technique to manipulate bifunctional DNA molecules: One end is thiolated to bind to a patterned gold surface and the other end is biotinylated to bind to a microtubule gliding over a kinesin-coated surface. We found that DNA molecules can be stretched and overstretched between the gold pads and the motile microtubules, and that they can form dynamic networks. This serves as a proof-of-principle that biological machineries can be used in vitro to accomplish the parallel formation of structured DNA templates that will have applications in biophysics and nanoelectronics.*

**Keywords:**
- DNA
- kinesin
- microtubules
- nanomanipulation

## 1. Introduction

DNA molecules are unique biological filaments, since they exhibit a small diameter, a high aspect ratio, and the capability for sequence-specific recognition and self-assembly. These properties make DNA molecules very promising candidates for the bottom-up construction of artificial structures in one, two, or three dimensions to be used in genomics,[1] biomolecular materials synthesis,[2] and nanoelectronics.[3] For example, 1) metallized DNA molecules[4–6] might provide a novel approach for the construction of nanoelectronic circuits, as silicon-based technology will face physical limits,[7] 2) surface-patterned DNA molecules will allow the setup of advanced DNA microarrays,[8,9] and 3) stretched DNA molecules will enable novel studies of DNA mechanics[10] and DNA–enzyme interactions.[11,12] However, in order to set up any of these systems, it is necessary to incorporate the DNA molecules into larger structures in a controlled manner.[4,13] This involves the specific attachment of the molecules to predefined locations as well as precise control over their structural conformation.[14] For individual molecules both requirements can be fulfilled by manipulation methods based on atomic force microscopy[15] and optical tweezers.[16] To manipulate many molecules in parallel, hydrodynamic flow[17–21] or molecular combing[22–25] can be used in combination with an end-specific attachment of DNA on chemically patterned surfaces.[4,13,26] However, flow manipulation and combing methods do not allow for the independent manipulation of molecules.

Recently, we showed that individual DNA molecules can be attached to microtubules gliding on kinesin-coated, unstructured surfaces.[27] We now explore whether this approach could be advanced to control the parallel, and yet individual manipulation of many DNA molecules in an engineered environment. The ends of λ-phage DNA (λ-DNA) were bifunctionalized with a thiol and biotin such that the thiolated end specifically attached to gold-coated surface regions. Once attached, the biotinylated ends of the DNA

[*] C. Z. Dinu,[+] Prof. Dr. J. Howard, Dr. S. Diez
Max Planck Institute of Molecular Cell Biology and Genetics
01307 Dresden (Germany)
Fax: (+49) 351-210-2020
E-mail: diez@mpi-cbg.de
Dr. J. Opitz,[+] Dr. M. Mertig
BioNanotechnology and Structure Formation Group
Max Bergmann Centre of Biomaterials
Dresden University of Technology, 01062 Dresden (Germany)
Fax: (+49) 351-463-39401
E-mail: mertig@tmfs.mpgfk.tu-dresden.de
Prof. Dr. W. Pompe
Institute of Materials Science
Dresden University of Technology, 01069 Dresden (Germany)
[+] C. Z. Dinu and J. Opitz contributed equally to this work.

Supporting information for this article is available on the WWW under http://www.small-journal.com or from the author.

small NANO MICRO

molecules were picked up, transported, and stretched by kinesin-driven microtubules. The bindings on both ends of the DNA were sufficiently strong that the molecules were stretched up to their full contour length and even beyond (i.e., overstretched[28]). Complex patterns and dynamic networks were formed, which may serve as templates for further metallization.[4,5,29]

## 2. Results

### 2.1. Bifunctionalization of λ-DNA with Thiol and Biotin

To achieve distinct binding of the two ends of the DNA molecules to different substrates, the single-stranded λ-DNA overhangs were specifically functionalized with a thiol and biotin by three Klenow polymerization reactions[30] (Figure 1a). The functionalization was designed such that in a first step (in the absence of dATP) the reaction stopped one base after incorporating two biotin-dCTP molecules at the right end of the DNA molecule (Figure 1a, I). In a second step (in the absence of dCTP), the reaction was stopped after incorporating one thiol-modified TTP group at the left end of the DNA molecule (Figure 1a, II). In the last step, the remaining DNA overhangs were filled with complementary unmodified phosphorylated bases (Figure 1a, III). The resulting λ-DNA molecules, which had one end thiolated (T) and the other end biotinylated (B), are denoted as T-DNA-B.

### 2.2. Two-Step Verification of the Specificity of End-Functionalization Reactions

First, to demonstrate the functionalization of one end of the DNA with biotin, T-DNA-B was bound to streptavidin-coated magnetic beads, precipitated with a magnet, and subsequently digested with *Hin*d III. After the digestion, the magnetic beads and their bound analytes were removed using a second magnetic precipitation. The remaining solution was subjected to gel electrophoresis (Figure 1b). While in the control of *Hin*d III-digested λ-DNA all fragments were visible, the 4 kb band was missing in the modified DNA. This result indicated that the biotinylated end of the DNA was removed together with the streptavidin-coated magnetic beads, whereas the thiolated end was not affected. Second, to demonstrate functionalization of the other end of the DNA with the thiol, T-DNA-B was bound to gold colloids (Figure 1c) and subjected to gel electrophoresis. In the gel, a broad DNA distribution ("smear") and a slightly shifted band to higher DNA fragment lengths was found (column 2). This can be attributed to the fact that several DNA molecules can bind to one gold colloid, leading to the formation of multicomplexes with reduced propagation

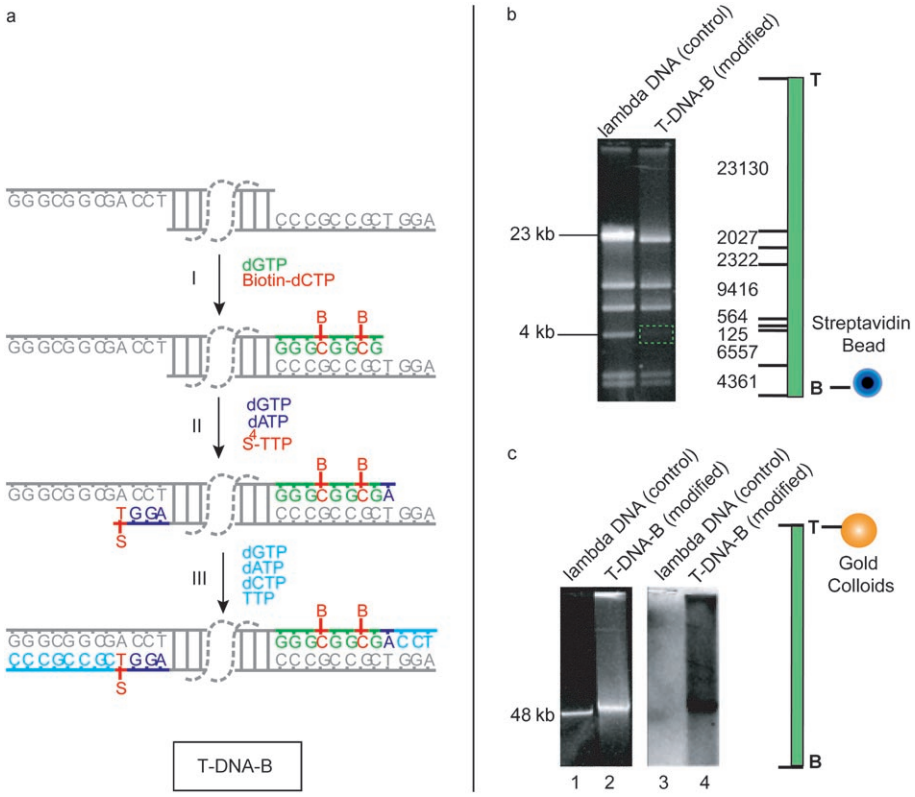


**Figure 1.** Bifunctionalization of λ-DNA molecules with a thiol and biotin. a) The functionalization of λ-DNA with biotin and a thiol was achieved through three Klenow polymerization reactions: I) Two biotin-modified bases were incorporated; II) a thiol-modified base was added; III) the remaining overhangs were filled with complementary unmodified bases. b) Confirmation of the biotin end-functionalization. T-DNA-B was bound to streptavidin-coated magnetic beads. The beads were then precipitated using a magnet and the attached DNA molecules were digested with *Hin*d III. Through a second magnetic precipitation, the supernatant was separated and run together with control λ-DNA digested with *Hin*d III (control). The digestion fragments are compared. The biotinylated end (4 kb fragment) is missing in the T-DNA-B column (highlighted band) proving the successful functionalization of the DNA with biotin. The fragments of the *Hin*d III-digested DNA are shown schematically on the right. c) Confirmation of the thiol end-functionalization. λ-DNA (column 1) and T-DNA-B (column 2) incubated with gold colloids are compared using gel electrophoresis. For T-DNA-B a broad distribution of the DNA is found due to the interaction of T-DNA-B with the gold colloids. This distribution becomes even more visible (black) when the same gel is stained using a gold enhancement technique[31] (columns 3 and 4).

  

in the gel. In contrast, control λ-DNA did not show any binding to the gold colloids (column 1). Thiol functionalization was further confirmed by staining the gel by using a gold-enhancement technique.[31] Here, the gold colloids bound to the T-DNA-B served as nucleation sites for growing larger gold particles, visible as black smear (column 3). Control λ-DNA did not show any reaction when subjected to gold enhancement (column 4).

### 2.3. Binding of T-DNA-B to Gold-Patterned Surfaces

The efficiency of DNA end functionalization was also evaluated by using a surface assay based on fluorescence microscopy. T-DNA-B was incubated for 30 min in a perfusion chamber containing patterned gold microstructures on glass. After the incubation, the unbound DNA was removed by washing with phosphate buffer (PB100) containing dimeric cyanine dye oxazole yellow (YOYO-1) and tris(2-carboxyethyl)phosphine (TCEP). Fluorescence images showed that individual T-DNA-B molecules were specifically attached to the gold surfaces (Figure 2a). In order to confirm the T-DNA-B attachment to gold by one end only, the bound molecules were stretched by applying a hydrodynamic flow (Figure 2b).

The surface coverage of T-DNA-B molecules was studied by using gold surfaces with feature sizes of $40\times40\ \mu m^2$ and varying the DNA incubation times. Using a T-DNA-B concentration of $700\ pg\,\mu L^{-1}$, it was found that $2.8\pm0.7$ (mean ± standard deviation) DNA molecules per $100\ \mu m^2$ were bound to the gold after 5-min incubation. The binding yield increased to $3.3\pm0.9$, $6.8\pm0.6$, $13.9\pm0.7$, and $14.7\pm0.7$ molecules per $100\ \mu m^2$ after 10, 15, 30, and 60 min, respectively. Apparently, the density of bound molecules approaches a saturation level of about 14 molecules per $100\ \mu m^2$ after 30 min. This density corresponds to a mean distance between the attached molecules of about 2.7 μm. This distance matches the extension of the measured trajectories of end-specifically conjugated quantum dots shown in Figure 2d. Thus, steric hindrance is presumably the reason for the observed saturation, and a 30-min incubation time was consequently chosen for the further experiments. The coverage of T-DNA-B on the glass surface was found to be $<0.1$ DNA molecules per $100\ \mu m^2$, independent of the incubation time.

Control experiments showed that neither control λ-DNA nor DNA biotinylated at both ends (B-DNA-B) bound to the gold surfaces (surface coverage $<0.1$ DNA molecules per $100\ \mu m^2$). In contrast, DNA molecules thiolated at both ends (T-DNA-T) readily bound to the gold pads on the surface. When a hydrodynamic flow was applied these molecules often stretched into an arched conformation, indicative of both ends being attached to the surface (Figure 2c).

The functionality of the biotinylated end of the T-DNA-B was checked after binding the thiolated end to the gold surface. Streptavidin-coated quantum dots (SA-Qdots) were allowed to bind to the biotinylated ends of the DNA in a perfusion chamber. In order to prevent nonspecific binding of the SA-Qdots to the surface, a blocking solution containing casein was applied after DNA incubation. Dual-color fluorescence micrographs were acquired using the FITC channel for the YOYO-1-labeled DNA and the TRITC channel for the SA-Qdots. It was found that SA-Qdots bound to about 80% of the attached T-DNA-B molecules (more than 200 molecules investigated). Specific binding to the biotinylated DNA ends was confirmed by the spatial fluctuations observed for the individual SA-Qdots representing the thermal motion of the DNA molecules by which they were tethered to the surface (Figure 2d and Movie S1 in the Supporting Information). Only a small number of SA-Qdots bound directly to the surface ($<3$ molecules per $100\ \mu m^2$), presumably due to insufficient surface blocking. No SA-Qdots were found to bind to T-DNA-T molecules.

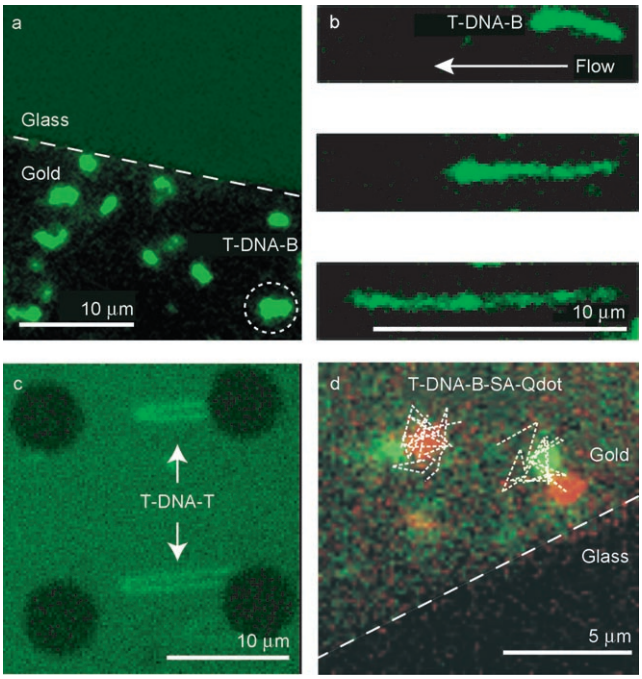


**Figure 2.** Binding of T-DNA-B to patterned gold surfaces. a) Fluorescence micrographs of YOYO-1-labeled T-DNA-B molecules (green) attached to a gold-patterned surface. The attached molecules exhibit a coiled conformation and undergo thermally driven motion. b) Hydrodynamic stretching of one T-DNA-B molecule (marked by the dotted circle in (a)) into a linear geometry. The hydrodynamic flow direction is indicated by the arrow; the three panels show the extension of the same T-DNA-B molecule at different time points under the influence of increasing flow speed. c) YOYO-1-labeled T-DNA-T bound to a patterned gold surface. When a flow is applied, the attached molecules assume an arched conformation (arrowheads). Here, imaging is performed through the substrate, hiding the actual binding sites of the thiolated DNA ends behind the gold. d) Binding of SA-Qdots (red) to the biotinylated ends of YOYO-1-labeled T-DNA-B (green). The thermally driven motion of the SA-Qdots attached to the biotinylated ends of the T-DNA-B were tracked and are shown by the white dotted lines.

  

small NANO MICRO

### 2.4. Stretching of T-DNA-B Molecules by Kinesin-Driven Microtubules

Kinesin-driven microtubules were employed to manipulate individual T-DNA-B molecules that were specifically attached to patterned gold surfaces. For this process, streptavidin was applied to the incubated T-DNA-B, and a kinesin-containing motor solution as well as a motility solution containing biotinylated rhodamine-labeled microtubules were subsequently flowed into the perfusion chamber.

The biotinylated microtubules, which moved on the kinesin-coated surface, bound to the streptavidin attached to the biotinylated end of the DNA (Figure 3a) and DNA stretching events occurred (Figure 3b and Movie S2 in the Supporting Information). A stretching event was defined as the observation of a DNA molecule that was stretched to at least a length of 10 μm by the action of a gliding microtubule.

76 stretching events that took place on the surface were analyzed over a field of view of $66 \times 66\ \mu m^2$. On average, $6 \pm 2$ stretching events over time periods of about 3 min were recorded. Imaging was continued until the linkage of the DNA disrupted either on the microtubule (70% of all stretching events) or on the gold (4%) or until the DNA molecule broke somewhere in-between (26%). Breakage of the DNA molecules along their lengths most likely resulted from photodamage[32] or mechanical stress, such as pipetting.[33] A detailed analysis of the final lengths of the stretched DNA molecules is shown in Figure 3c. As shown, most of the molecules reach a length above the contour length of λ-DNA (estimated at 18.6 μm[20] for the amount of YOYO-1 used in these experiments). These observations show that: 1) the forces of the motors were high enough to fully stretch (and even overstretch) the DNA molecules, and 2) the gold–thiol bond was strong enough to withstand the associated forces. Only in a small percentage, the bonds broke at the gold site or in very close proximity.

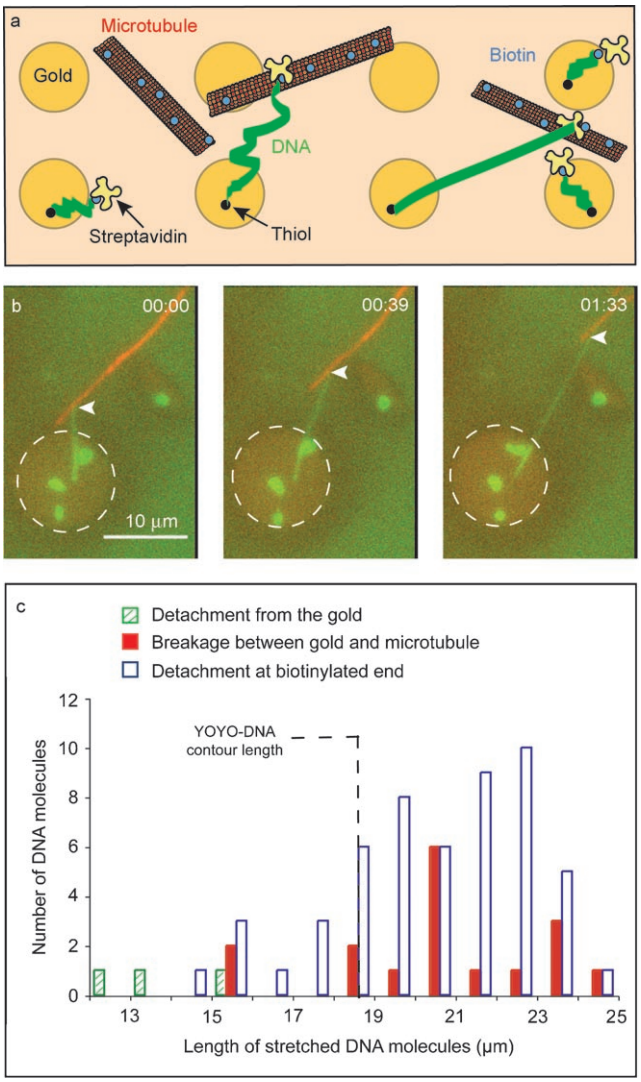


**Figure 3.** Stretching of T-DNA-B by kinesin-driven microtubules. a) Schematic diagram of the specific attachment of T-DNA-B to the complementary surfaces. The thiolated end of the DNA binds specifically to the gold pads. The biotinylated DNA end binds to a biotinylated microtubule via a streptavidin linkage. Using the forces developed by the kinesin molecules, the microtubules stretch the DNA molecules to linear geometries. b) Fluorescence micrographs of a time series [min:s] showing the stretching of a YOYO-1-labeled DNA molecule (green) by a motile rhodamine-labeled microtubule (red). The length to which the molecule was stretched is about 20 μm. c) Histogram of DNA molecules as a function of their final stretching length ($N = 76$). All events are categorized as follows: detachment from the gold (green), detachment from the microtubule (blue), breakage between the gold and the microtubule (red).

### 2.5. Parallel DNA Manipulation on Periodically Arranged Gold Patterns

Regularly patterned surfaces with 10-μm gold pads arranged in a quadratic geometry were used to demonstrate the simultaneous occurrence of DNA stretching events (Figure 4 and Movies S3 and S4 in the Supporting Information). Figure 4a illustrates the parallel manipulation of individual DNA molecules bound to adjacent gold pads by kinesin-driven microtubules. The DNA molecules were stretched from the pads to the glass surfaces in independent directions.

Figure 4b shows one T-DNA-B molecule (DNA 1), which was picked up and pulled from the lower-left gold pad over to the upper-left pad reaching a length of 22 μm. After the microtubule-attached end of DNA 1 crossed the upper pad, a second DNA molecule (DNA 2) was stretched diagonally from the upper-left towards the lower-right pad. This molecule attained a total length of 24 μm (not shown). The stretching events in this example show that the gold-patterned surface neither influenced the microtubule motility nor the pulling of the DNA over the edges of the micropatterned gold pads.

Figure 4c shows an example where a DNA molecule is stretched between a gold pad and a motile microtubule in a spool-like conformation. Such microtubule spools form spontaneously on kinesin-coated surfaces in the presence of crosslinking molecules (such as biotin–streptavidin).[34,35]

  

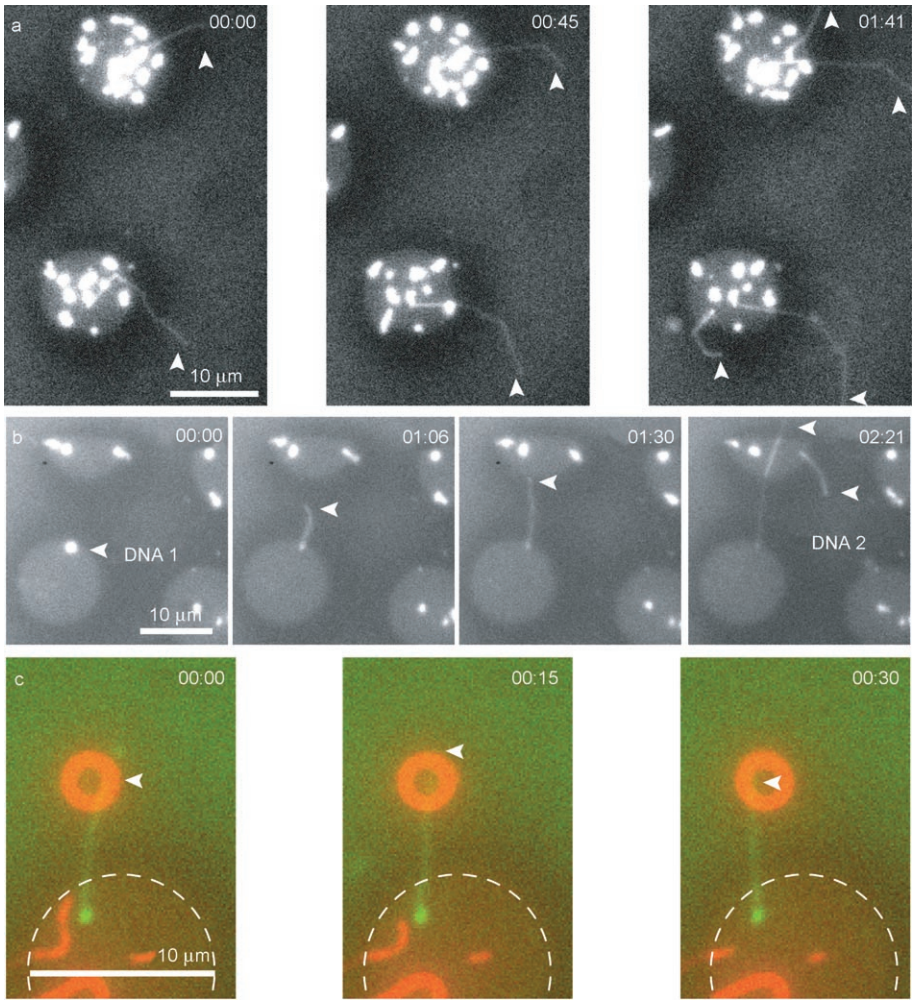


**Figure 4.** DNA stretching on periodically arranged gold pads. a) Fluorescence micrographs showing the stretching of several YOYO-1-labeled T-DNA-B molecules (FITC channel) on a patterned gold surface with 10-μm feature size. Driven by the force exerted by the kinesin, the microtubules (which were also imaged but are not shown) stretch the DNA molecules to linear geometries. Some of the DNA molecules are bent due to weaving around motile microtubules. b) YOYO-1-labeled DNA molecules are manipulated by gliding microtubules (not shown) in such a way that linear geometries are formed. The arrows point to the DNA molecules that were stretched by the microtubules. c) Fluorescence micrographs showing a rhodamine-labeled microtubule (red) in a spool-like conformation rotating in place and periodically stretching a YOYO-1-labeled T-DNA-B molecule (green). The dashed line indicates the location of the gold pad and the arrows indicate the attachment points of the T-DNA-B to the microtubule. (The time in all images is given in [min:s])

The result is a rotary motion of the spool generated by the action of linear motors. In our example, the rotary motion leads to a periodic stretching and unstretching of the DNA molecule (see Movie S5 in the Supporting Information). Before the image recording had started, the DNA molecule was already stretched to about 10 μm while attached to the spool. The event was imaged up to the time where the DNA was broken. During this time, the spool was stable enough to accommodate continuous rotation.

These examples demonstrate the principal feasibility of parallel and yet individual DNA stretching events between periodically arranged microstructures as well as the bifunctional coupling of DNA molecules to more intricate motility systems. In order to use the system for the generation of regular DNA networks, appropriate techniques to attach the stretched DNA molecules to the target structures need to be developed. This is a subject for further research, beyond the scope of this paper.

### 2.6. Dynamic Interactions between Stretched DNA Molecules

Another example of the simultaneous manipulation of multiple DNA molecules by the molecular motors is given in Figure 5 (see also Movie S6 in the Supporting Information). The intricate network was formed on top of 40 × 40 μm$^2$ gold squares by the activity of kinesin-driven microtubules on three DNA molecules.

Already before our image recording had started, DNA molecule 1 (DNA 1, shown in green) had been stretched to about 22 μm and bound nonspecifically to the surface such that its ends remained at fixed locations. A second DNA molecule (DNA 2, blue) was stretched to a length of about 20 μm by the action of a motile microtubule (microtubule A). It was then disrupted from microtubule A and reattached to microtubule B, which had a different direction of movement. After being stretched to a final length of about 22 μm, the molecule detached from microtubule B and returned to its attachment point undergoing thermally driven motion. A third DNA molecule (DNA 3, red) was looped around DNA 1 approximately in the middle. Microtubule C stretched DNA 3 first towards the right, leading to an increasing kink in DNA 1 caused by a DNA–DNA interaction. After microtubule C changed its direction towards the left, DNA 1 and DNA 3 were eventually disentangled.

We identified DNA–DNA interactions where two stretched molecules were woven into Y-type crossings (see, for example, the middle image on the upper panel of Figure 5) and X-type crossings, where the two stretched DNA molecules crossed over each other (see, for example, the middle image on the lower panel of Figure 5). We ob-

  

small NANO MICRO

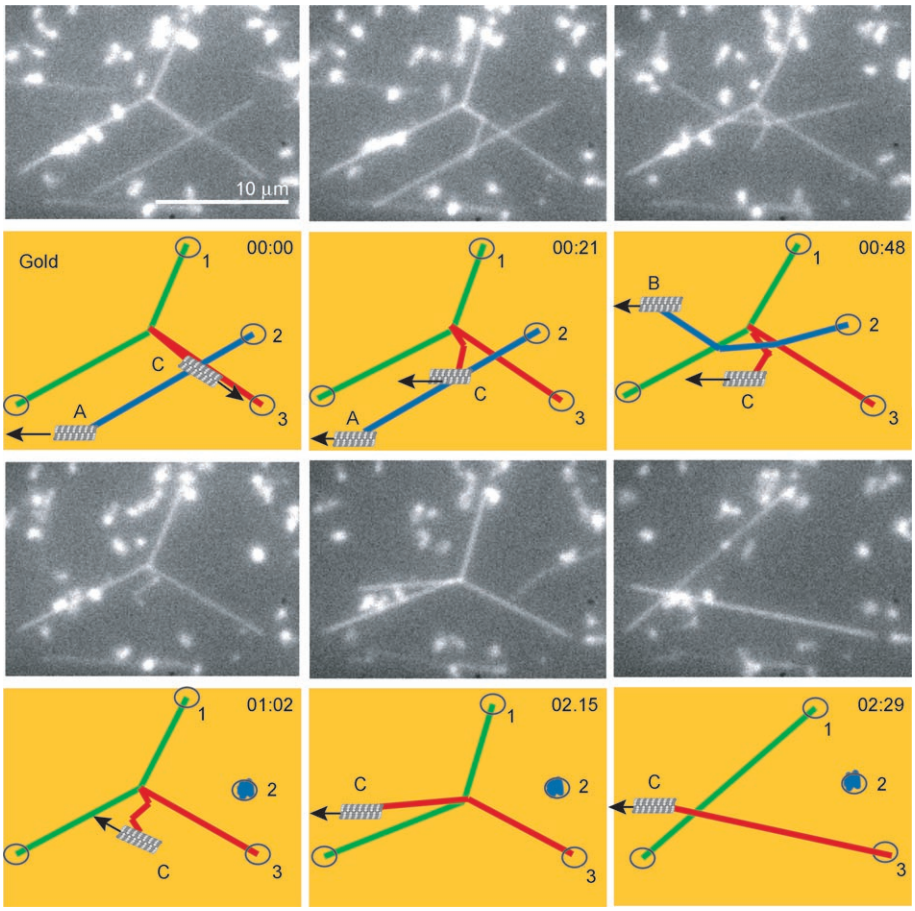


**Figure 5.** Dynamic interactions between stretched DNA molecules. Fluorescence micrographs of YOYO-1-labeled DNA molecules bound and stretched on a gold surface and schematic interpretations deduced from the full video sequence (time shown in [min:s]). In the stretching events shown here, the DNA molecules are woven together to form loops and junctions by motile microtubules (shown in the drawings). Different DNA molecules are shown in different colors.

served a number of additional networks simultaneously formed by multiple DNA molecules.

## 3. Discussion

We have shown in a cell-free environment that individual bifunctionalized T-DNA-B molecules can be specifically attached with the thiolated end to micropatterned gold surfaces while the biotinylated ends are picked up and manipulated by kinesin-driven microtubules. Using the forces generated by the motors, we observed parallel and yet individual DNA stretching events, DNA–DNA interactions, and dynamic network formation.

Binding the thiolated end of T-DNA-B to gold surfaces (instead of using complementary oligonucleotides or thiol derivates of biotin[18]) yields several advantages. First, no additional surface functionalization is necessary, and secondly, a high force resistance in stretching is obtained.[13] We verified that our system is well defined by specifically attaching streptavidin coated quantum dots to the biotinylated ends of the DNA.

We specifically manipulated individually attached DNA molecules by using kinesin-driven microtubules and investigated the mechanical stability of the DNA molecules. Because a high density of kinesin motors was used (>3000 $\mu m^{-2}$), the generated force[36] was large enough to stretch and even overstretch individual DNA molecules.[10,27,28] Stretching up to 150% of the contour length of λ-DNA was observed prior to detachment or breakage. However, due to the large influence of the fluorescence labeling on the molecular elasticity of the DNA,[37–40] it is not straightforward to determine the stretching forces generated by the motile microtubules. For example, common force–distance measurements on unstained λ-DNA molecules reveal a characteristic plateau at 65 pN[10,28,41] followed by an abrupt extension before the duplex unbinds at forces of about 150 pN.[42] In contrast, a considerable shift of the overstretching transition to higher forces, and thus the disappearance of the 65-pN plateau, when the intercalator YOYO-1 is used as fluorescence dye was reported.[40] However, this particular result cannot be used for a quantitative analysis of our experiment, since we labeled the DNA at a much lower dye-to-nucleotide ratio. Therefore, thorough investigation of the influence of YOYO-1 on the entropic and mechanical properties of DNA is necessary to further evaluate the observed stretching events. Once the detailed force–extension curve of the utilized DNA molecules is known, new possibilities for studying both DNA duplex elastic behavior and the collective behavior of the kinesin motor action[43] will arise. Nevertheless, conceptually similar to earlier demonstrations,[44,45] our DNA-stretching experiments show that it is possible to carry out biophysical investigations where all the involved components – including force generation and detection – work autonomously at the molecular level.

It was also possible to quantify the number of DNA rupture events upon stretching. 70% of the stretched DNA molecules detached at the microtubules suggesting that the connection between the DNA and the gold substrate is

  

stronger than the one between the DNA and the microtubule. This observation is in accordance with the reported energy of the streptavidin–biotin single-ligand receptor being 96 kJ mol$^{-1}$,[46,47] while the thiol–gold interaction is 167 kJ mol$^{-1}$.[48,49] Although in our experiments two biotins on the microtubule and two biotins on the DNA could potentially form bonds with streptavidin, most likely only one bond was formed, partially due to steric hindrance. Any nonspecific binding energy of DNA via phosphate moieties is on the order of a few kJ mol$^{-1}$.[49,50] Moreover, one has to take into account that our experiments were carried out on a second or minute time scale, and therefore the unbinding force is lower than that required for a faster pulling. These results also show that the force developed by kinesin on the microtubule tracks can compete with the biotin–streptavidin breaking force.[51] We suppose the interest of such a method lies in the possibility to nondestructively exert and measure forces on other biological ligands or even artificial polymers using the same geometry.

Our molecular manipulation technique permitted the alignment and stretching of DNA molecules on the gold-patterned surfaces. We were able to manipulate many DNA molecules simultaneously and to assemble DNA networks. An interesting extension will be the construction of multidimensional DNA networks, for which microtubule motility and DNA-attachment needs to be guided in a three-dimensional manner.[52]

Although not demonstrated here, the dynamic DNA networks observed in our experiments can be stabilized at any time by stopping the microtubule movement.[21,53–55] Therefore, the described network formation can be seen as an engineering analogue to the basic biological principle of structural evolution. In cells, the structures are continuously formed by assembling and disassembling complex units, by selecting and stabilizing these units through the recruitment of additional proteins.

## 4. Conclusions

This report illustrates a new strategy for designing and preparing complex patterns of DNA molecules on engineered surfaces. The highly specific binding and the parallel yet individual manipulation of DNA molecules by means of kinesin-driven microtubules is expected to be useful for nanotechnology as well as for biophysical studies. The resulting DNA structures serve as a proof-of-principle that biological motors can be used in molecular manufacturing.

## 5. Experimental Section

*Substrate preparation*: Patterned gold surfaces were prepared on glass cover slips (Corning, US) by evaporation. TEM grids with 400 lines per inch (Plano GmbH, Germany) and hole grids with 6.5 μm and 10 μm hole diameters and a center-to-center spacing of 19 μm and 20 μm, respectively, were used as masks. The film thickness was typically 90 nm for the 40-μm pads and 230 nm for the 10- and 6.5-μm pads.

Glass cover slips and patterned gold surfaces were cleaned by sequential immersion in fuming nitric acid (100%, 1 min for the 40-μm pads and 20 s for the 10-μm and 6.5-μm pads) and a neutralization solution (hydrogen peroxide (30 wt% in water; Sigma, Germany), ammonium hydroxide (28–30 wt% in water; Acros Organics, Germany) and water in a 1:1:5 ratio) for 5 min and 2.5 min, respectively. The neutralized surfaces were soaked, extensively rinsed, and stored in water.

All experiments were performed in 100-μm-thick perfusion chambers of about 40 μL volume, built from cleaned cover glasses and cleaned patterned gold surfaces separated by a double-sided tape spacer.[56]

*End-labeling of the λ-DNA*: λ-phage dsDNA (λ-DNA; New England Biolabs Inc., UK) was used, containing 48 502 base pairs. In its native form, it has a contour length of about 16.5 μm. The molecule contains 12-base-long, single-stranded overhangs at both ends that are self-complementary. To properly resolve the DNA end-labeling, the samples were heated up to 65 °C so that any circular closed molecules were melted. Functionalization was carried out in three Klenow polymerization reactions. In a first step, dGTP (Sigma, Germany) and Biotin-14-dCTP (Gibco, Germany) were incorporated using DNA polymerase I, large Klenow fragment (New England Biolabs) in NEB2 buffer (10 mM Tris-HCl, 50 mM NaCl, 10 mM $MgCl_2$, 1 mM dithiothreitol, pH 7.9, 25 °C; New England Biolabs). For this, the mixture was incubated at 25 °C for 25 min (activation of the enzyme) followed by 75 °C for 10 min (inactivation of the enzyme). In the absence of dATP the reaction stopped at the TTP position. The DNA was loaded for purification in a Microcon YM-100 filter (Millipore, Germany) and centrifuged at 500 g. By inverting the filter, the purified DNA was recovered. In the second step, dATP (Sigma, Germany), dGTP, $S^4$-TTP (4-thiothymidine triphosphate, TriLink BioTechnologies, US) were incorporated using Klenow fragment (3′→5′ exo$^-$; New England Biolabs). The processes of incorporation, filtration, and recovery were performed as described above. The third step consisted of filling up the remaining overhangs with dCTP, TTP, dATP, and dGTP. The final purification step exchanged the NEB2 buffer for phosphate buffer PB100 (a mixture of sodium phosphate monobasic and sodium phosphate tribasic (Sigma, Germany), 100 mM, pH 7.5). The purified DNA was recovered by centrifugation at 1000 g.

DNA was also labeled with thiol or biotin at both ends (T-DNA-T and B-DNA-B, respectively). For T-DNA-T, Klenow fragment (3′→5′ exo$^-$) in NEB2 buffer and dATP, dGTP, $S^4$-TTP and dCTP were added. For the B-DNA-B, large Klenow fragment in NEB2 and Biotin-dCTP, dATP, dGTP, TTP were used. The DNA was purified and recovered as described above.

The efficiency of the functionalization reactions were checked by using gel electrophoresis. 1) 0.1 μg of T-DNA-B was bound to streptavidin-coated magnetic beads (Dynal, Germany) by incubation of the sample at room temperature overnight. The beads were then precipitated using a magnet and unbound molecules were removed by rinsing with buffer solution. The DNA molecules bound to the beads were digested with *Hin*d III (New England Biolabs). The supernatant was separated again using a magnet and run in a 0.5% agarose gel (Seakem Gold; Biozym, Germany) together with the control λ-DNA *Hin*d III digested, for 1.5 h, at

  

NANO MICRO small

80 V. The gel was stained with SYBR Green (Molecular Probes, UK) in TAE (tris-acetate) buffer for 5 min. 2) 0.2 μg of T-DNA-B and 0.2 μg of λ-DNA were bound to gold colloids (5-nm diameter; Sigma, Germany) by incubation of the sample at room temperature overnight. After incubation, the samples were run in a 0.5% agarose gel. First, the gel was stained with SYBR Green and imaged. Subsequently, the gel was restained using a gold-enhancement technique. For this, $KAuCl_4$ (600 μL, 23 mg mL$^{-1}$; Sigma, Germany) was mixed with KSCN (600 μL, 60 mg mL$^{-1}$; Sigma, Germany) followed by centrifugation at 5000 g for 1 min. The pellet was dissolved in 4800 μL of 1 M sodium phosphate buffer (pH 5.5; Sigma, Germany). Then, 1200 μL of hydrochinone (5.5 mg mL$^{-1}$; Sigma, Germany) were added. The gel was incubated with the solution for 15 min, subsequently rinsed with water, and imaged.

Bulk studies were used to check the efficiency of the end-labeling of DNA with the thiol and biotin. YOYO-1 iodide ($\lambda_{exc}$ = 491 nm; $\lambda_{em}$ = 509 nm; 1 mM solution in DMSO; Molecular Probes, UK) was incubated with T-DNA-B at 37 °C for 2 h in a ratio of eight nucleotides per dye molecule. Thereafter the DNA was flowed into the perfusion chamber and kept in a humidified atmosphere. After an incubation time of 5, 10, 15, 30, and 60 min the chamber was rinsed with 100 μL of PB100 to remove unbound molecules. Subsequently, the perfusion chamber was incubated with a casein solution for 5 min (0.5 mg mL$^{-1}$ in PB100; Sigma, Germany). Next, a solution containing streptavidin-covered quantum dots (SA-Qdots; 605 nm emission, 8 nM; Quantum Dot Corporation, US) was added. The SA-Qdots were allowed to bind for 5 min. Any unbound molecules were removed with PB100-containing TCEP reducing agent (tris(2-carboxyethyl)-phosphine, 100 mM; Molecular Probes, UK). The specific binding of DNA to gold and to SA-Qdots was observed using fluorescence microscopy. The number of bound molecules per μm$^2$ was quantified. As controls, T-DNA-T and B-DNA-B were used as described above.

*Motility assay*: A mixture of rhodamine tubulin, biotin tubulin, and tubulin (Cytoskeleton, US) in a ratio of 3:4:9 and a total concentration of 4 mg mL$^{-1}$ was polymerized at 37 °C in BRB80 buffer (80 mM Pipes, pH 6.8 with KOH, 1 mM $MgCl_2$, 1 mM EGTA) enriched by 5% DMSO, 4 mM $MgCl_2$, and 1 mM Mg-GTP (Sigma, Germany). The solution was diluted 100 times in BRB80 with 10 mM taxol. Dimeric full-length wild-type *Drosophila melanogaster* kinesin (from the pPK113 plasmid) with the 6-histidine tagged, expressed in *Escherichia coli* was purified as described elsewhere.[55] The motility assay was adapted after a standard protocol.[56] Briefly, the perfusion chamber was incubated with T-DNA-B for 30 min at room temperature. The unbound DNA molecules were removed with PB100. Subsequently, a solution containing streptavidin (8 nM; Pierce, Germany) was added. The streptavidin was allowed to bind for 5 min. Next, the surfaces of the perfusion chamber were blocked with a casein solution for 5 min (0.5 mg mL$^{-1}$ in PB100; Sigma, Germany) followed by the motor-containing solution (10 μg mL$^{-1}$ kinesin with 1 mM ATP and 0.2 mg mL$^{-1}$ casein in PB100). The motors were allowed to bind for 5 min. In the last step, a motility solution containing rhodamine-labeled biotinylated microtubules (32 nM tubulin dimer), 0.2 mg mL$^{-1}$ casein, 10 μM taxol, 1 mM ATP, the anti-fade solution containing 0.02 mg mL$^{-1}$ catalase, 0.02 mM glucose oxidase, 0.02 mM D-glucose (Sigma, Germany), 10 mM TCEP, and YOYO-1 (1 dye per 8 nucleotides) were added. The speed of the DNA-loaded gliding microtubules ranged from about 0.18–0.3 μm s$^{-1}$.

*Fluorescence microscopy and imaging*: The perfusion chamber was mounted on an inverted fluorescence microscope Axiovert 200M (Zeiss, Germany). A high-magnification (100×, N.A. = 1.3) oil-immersion objective and the appropriate blue (FITC) and green (TRITC) optical filter sets were used to image the DNA molecules, SA-Qdots, and microtubules. Images were acquired using a 16-bit cooled frame-transfer CCD camera (Micromax, 512 BFT; Visitron, Germany) with 100-ms exposure times and captured on a computer using Metamorph imaging software (Visitron). Dual-color images at 3-s time intervals were obtained by interchanging the filter sets between sequential acquisition.

## Acknowledgements

*We would like to thank Jonne Helenius for his support. J.O. and M.M. gratefully acknowledge Li Yixuan and Rizwan Ali for their help on the DNA functionalization and Jan Voigt for preparing the micropatterned gold surfaces. The work was financially supported by the BMBF (contracts: 03I4025 A and 03N8712) and the DFG (FG 335/TPB4). M.M. acknowledges partial support from the DFG (contract: ME 1256/7).*

[1] C. A. Mirkin, *Inorg. Chem.* **2000**, *39*, 2258.
[2] N. C. Seeman, *Nature* **2003**, *421*, 427.
[3] H. Yan, S. H. Park, G. Finkelstein, J. H. Reif, T. H. LaBean, *Science* **2003**, *301*, 1882.
[4] E. Braun, Y. Eichen, U. Sivan, G. Ben-Yoseph, *Nature* **1998**, *391*, 775.
[5] M. Mertig, C. L. Colombi, R. Seidel, W. Pompe, A. De Vita, *Nano Lett.* **2002**, *2*, 841.
[6] J. Richter, M. Mertig, W. Pompe, H. Vinzelberg, *Appl. Phys. A* **2002**, *74*, 725.
[7] M. Berciu, T. G. Rappoport, B. Janko, *Nature* **2005**, *435*, 71.
[8] G. Ramsay, *Nat. Biotechnol.* **1998**, *16*, 40.
[9] M. Gad, S. Sugiyama, T. Ohtani, *J. Biomol. Struct. Dyn.* **2003**, *21*, 387.
[10] C. Bustamante, Z. Bryant, S. B. Smith, *Nature* **2003**, *421*, 423.
[11] R. J. Davenport, G. J. Wuite, R. Landick, C. Bustamante, *Science* **2000**, *287*, 2497.
[12] A. Goel, R. D. Astumian, D. Herschbach, *Proc. Natl. Acad. Sci. USA* **2003**, *100*, 9699.
[13] Y. Zhang, R. H. Austin, J. Kraeft, E. C. Cox, N. P. Ong, *Phys. Rev. Lett.* **2002**, *89*, 198102.
[14] M. Mertig, W. Pompe in *Nanobiotechnology: Concepts, Applications and Perspectives* (Eds.: C. M. Niemeyer, C. A. Mirkin), Wiley-VCH, Weinheim, **2004**, pp. 256–277.
[15] D. Nyamjav, A. Ivanisevic, *Adv. Mater.* **2003**, *15*, 1805.
[16] U. Bockelmann, P. Thomen, B. Essevaz-Roulet, V. Viasnoff, F. Heslot, *Biophys. J.* **2002**, *82*, 1537.
[17] M. Mertig, L. Colombi Ciacchi, A. Benke, A. Huhle, J. Opitz, R. Seidel, H. K. Schackert, W. Pompe in *Foundations of Nanoscience: Self-Assembled Architectures and Devices* (Ed.: J. Reif), *Science Technica*, **2004**, pp. 132–145.
[18] R. M. Zimmermann, E. C. Cox, *Nucleic Acids Res.* **1994**, *22*, 492.
[19] T. T. Perkins, S. R. Quake, D. E. Smith, S. Chu, *Science* **1994**, *264*, 822.

  

[20] P. S. Doyle, B. Ladoux, J. L. Viovy, *Phys. Rev. Lett.* **2000**, *84*, 4769.
[21] F. Gast, P. Dittrich, P. Schiwille, M. Weigel, M. Mertig, J. Opitz, U. Queitsch, S. Diez, B. Lincoln, F. Wottawah, S. Schinkinger, J. Guck, J. Kas, J. Smolinski, K. Salchert, C. Werner, C. Duschl, M. Jager, K. Uhlig, P. Geggier, S. Howitz, *Microfluid Nanofluid* **2006**, *2*, 21.
[22] A. Bensimon, A. Simon, A. Chiffaudel, V. Croquette, F. Heslot, D. Bensimon, *Science* **1994**, *265*, 2096.
[23] J. F. Allemand, D. Bensimon, L. Jullien, A. Bensimon, V. Croquette, *Biophys. J.* **1997**, *73*, 2064.
[24] K. Otobe, T. Ohtani, *Nucleic Acids Res.* **2001**, *29*, E109.
[25] P. Bjork, A. Herland, I. Scheblykin, O. Ingana, *Nano Lett.* **2005**, *5*, 1948.
[26] J. Opitz, F. Braun, R. Seidel, W. Pompe, B. Voit, M. Mertig, *Nanotechnology* **2004**, *15*, 717.
[27] S. Diez, C. Reuther, C. Dinu, R. Seidel, M. Mertig, W. Pompe, J. Howard, *Nano Lett.* **2003**, *3*, 1251.
[28] C. Bustamante, J. Marko, E. Siggia, S. Smith, *Science* **1994**, *265*, 1599.
[29] G. A. Burley, J. Gierlich, M. R. Mofid, H. Nir, S. Tal, Y. Eichen, T. Carell, *J. Am. Chem. Soc.* **2006**, *128*, 1398.
[30] V. Derbyshire, P. S. Freemont, M. R. Sanderson, L. Beese, J. M. Friedman, C. M. Joyce, T. A. Steitz, *Science* **1988**, *240*, 199.
[31] R. Seidel, L. Colombi Ciacchi, M. Weigel, W. Pompe, M. Mertig, *J. Phys. Chem. B* **2004**, *108*, 10801.
[32] B. Akerman, E. Tuite, *Nucleic Acids Res.* **1996**, *24*, 1080.
[33] C. Storm, P. C. Nelson, *Phys. Rev. E* **2003**, *67*, 051906.
[34] H. Hess, J. Clemmens, C. Brunner, R. Doot, S. Luna, K. H. Ernst, V. Vogel, *Nano Lett.* **2005**, *5*, 629.
[35] M. Bachand, A. M. Trent, B. C. Bunker, G. D. Bachand, *J. Nanosci. Nanotechnol.* **2005**, *5*, 718.
[36] J. Howard, A. Hudspeth, R. Vale, *Nature* **1989**, *342*, 154.
[37] S. Quake, H. Babcock, S. Chu, *Nature* **1997**, *388*, 151.
[38] M. L. Bennink, O. D. Scharer, R. Kanaar, K. Sakata-Sogawa, J. M. Schins, J. S. Kanger, B. G. de Grooth, J. Greve, *Cytometry* **1999**, *36*, 200.
[39] R. Eckel, R. Ros, A. Ros, S. Wilking, N. Sewald, D. Anselmetti, *Biophys. J.* **2003**, *85*, 1968.
[40] A. Sischka, K. Toensing, R. Eckel, S. Wilking, N. Sewald, R. Ros, D. Anselmetti, *Biophys. J.* **2005**, *88*, 404.
[41] I. Rouzina, V. A. Bloomfield, *Biophys. J.* **2001**, *80*, 894.
[42] H. Clausen-Schaumann, M. Rief, C. Tolksdorf, H. Gaub, *Biophys. J.* **2000**, *78*, 1997.
[43] S. Klumpp, R. Lipowsky, *Proc. Natl. Acad. Sci. USA* **2005**, *102*, 17284.
[44] H. Hess, J. Howard, V. Vogel, *Nano Lett.* **2002**, *2*, 1113.
[45] F. Gittes, E. Meyhöfer, J. Howard, *Biophys. J.* **1996**, *70*, 418.
[46] E. L. Florin, V. T. Moy, H. E. Gaub, *Science* **1994**, *264*, 415.
[47] B. Isralewitz, M. Gao, K. Schulten, *Curr. Opin. Struct. Biol.* **2001**, *11*, 224.
[48] A. Ulman, *Chem. Rev.* **1996**, *96*, 1533.
[49] A. B. Steel, R. L. Levicky, T. M. Herne, M. J. Tarlov, *Biophys. J.* **2000**, *79*, 975.
[50] M. D. Porter, T. B. Bright, D. L. Allara, C. E. D. Chidseyi, *J. Am. Chem. Soc.* **1987**, *109*, 3559.
[51] O. Taisuke, T. Suguira, N. Ikoma, *Appl. Phys. Lett.* **2005**, *87*, 043901.
[52] G. Romet-Lemonne, M. VanDuijn, M. Dogterom, *Nano Lett.* **2005**, *5*, 2350.
[53] B. J. Schnapp, B. Crise, M. P. Sheetz, T. S. Reese, S. Khan, *Proc. Natl. Acad. Sci. USA* **1990**, *87*, 10053.
[54] T. U. Mayer, T. M. Kapoor, S. J. Haggarty, R. W. King, S. L. Schreiber, T. J. Mitchison, *Science* **1999**, *286*, 971.
[55] D. L. Coy, W. O. Hancock, M. Wagenbach, J. Howard, *Nat. Cell Biol.* **1999**, *1*, 288.
[56] J. Howard, A. J. Hunt, S. Baek, *Methods Cell Biol.* **1993**, *39*, 137.

Received: March 7, 2006
Published online on June 21, 2006

  